Cell, Vol. 109, 769–779, June 14, 2002, Copyright ©2002 by Cell Press

A DEAD-Box Protein Functions as an ATP-Dependent RNA Chaperone in Group I Intron Splicing

Sabine Mohr, John M. Stryker, and Alan M. Lambowitz[1]
Institute for Cellular and Molecular Biology
Department of Chemistry and Biochemistry
Section of Molecular Genetics and Microbiology
School of Biological Sciences
University of Texas at Austin
Austin, Texas 78712

Summary

The *Neurospora crassa* CYT-18 protein, the mitochondrial tyrosyl-tRNA synthetase, functions in splicing group I introns by inducing formation of the catalytically active RNA structure. Here, we identified a DEAD-box protein (CYT-19) that functions in concert with CYT-18 to promote group I intron splicing in vivo and vitro. CYT-19 does not bind specifically to group I intron RNAs and instead functions as an ATP-dependent RNA chaperone to destabilize nonnative RNA structures that constitute kinetic traps in the CYT-18-assisted RNA-folding pathway. Our results demonstrate that a DExH/D-box protein has a specific, physiologically relevant chaperone function in the folding of a natural RNA substrate.

Introduction

Group I and group II introns use RNA-catalyzed splicing mechanisms but require proteins for efficient splicing in vivo to help fold the intron RNAs into the catalytically active structure (reviewed in Lambowitz et al., 1999). Several group I and group II intron splicing factors studied biochemically have been shown to bind specifically to the intron RNAs and either induce the formation of the catalytically active RNA structure, promote splicing by an alternative tertiary structure-capture mechanism, or use some combination of the two mechanisms. These protein-assisted splicing reactions have provided insight into how proteins mediate RNA folding and RNA-catalyzed reactions as well as the evolution of splicing mechanisms.

In addition to proteins that bind specifically to the intron RNAs, it has been suggested that nonspecific RNA binding proteins may also facilitate group I and group II intron splicing by functioning as RNA chaperones to alleviate "kinetic traps" (Herschlag, 1995; Woodson, 2000). Such kinetic traps are endemic to group I and group II intron folding pathways due to the propensity of the highly structured intron RNAs to form stable nonnative secondary and tertiary structures. Several proteins that bind RNA nonspecifically, including *Escherichia coli* StpA and ribosomal protein S-12, were shown to have an "RNA chaperone activity" that stimulates splicing of the phage T4 *td* intron in vitro or when overexpressed in vivo (Coetzee et al., 1994; Zhang et al., 1995; Clodi et al., 1999). It remains unclear, however, whether these proteins normally function as RNA chaperones. In yeast, mutations in the nuclear gene *MSS116*, which encodes a DEAD-box protein, inhibit splicing of a number of mitochondrial (mt) group I and group II introns (Séraphin et al., 1989). Overexpression of Mss116p increases the ATP-dependent splicing of the group II intron bI1 in mt lysates (Niemer et al., 1995), but a direct role for Mss116p in the splicing reaction has not been demonstrated.

The DExH/D-box proteins are a large family of ATPases that have been proposed to mediate RNA structural rearrangements in a variety of cellular processes, including nuclear pre-mRNA splicing, ribosome assembly, protein synthesis, nuclear transport, and RNA degradation (Tanner and Linder, 2001). Studies with artificial substrates have shown that some DExH/D box proteins have RNA helicase activity and can disrupt RNA/protein interactions, and they are postulated to function similarly on natural substrates (Jankowsky et al., 2000, 2001). The involvement of DExH/D-box proteins in group I and group II intron splicing would be a potential evolutionary link to spliceosomal introns, where such proteins are proposed to mediate structural rearrangements at multiple steps in the splicing process.

The *Neurospora crassa* mt tyrosyl-tRNA synthetase or CYT-18 protein, the first group I intron splicing factor to be identified, functions in splicing several mt group I introns (Mannella et al., 1979; Akins and Lambowitz, 1987; Wallweber et al., 1997). The CYT-18 protein promotes splicing by recognizing conserved tRNA-like structural features of group I introns and inducing formation of RNA tertiary structure required for catalytic activity (Caprara et al., 1996a, 1996b; Myers et al., 2002). The group I intron catalytic core consists of two extended double-helical domains, one formed by the coaxial stacking of secondary structure elements P5, P4, and P6, and the other formed by P3, P8, P7, and P9, with the juxtaposition of the two domains creating a cleft that contains the intron's active site (Michel and Westhof, 1990; Golden et al., 1998). Biochemical and genetic studies have led to a model in which CYT-18 binds first to the P4-P6 domain to promote its assembly and then makes secondary contacts with the P3-P9 domain to stabilize the two domains in the correct relative orientation to form the intron's active site (Caprara et al., 1996a, 1996b).

Although CYT-18 is by itself sufficient to promote the splicing of the *N. crassa* mt group I introns in vitro, the purified protein functions efficiently at 37°C but not at the normal growth temperature of 25°C, suggesting that one or more additional proteins are needed to overcome a step with a high activation enthalpy. In addition to *cyt-18*, the initial genetic screens showed that mutations in two other nuclear genes, *cyt-4* and *cyt-19*, cause defective group I intron splicing in vivo (Bertrand et al., 1982). The *cyt-4* gene encodes a protein homologous to *E. coli* RNase II and likely functions in RNA turnover, with *cyt-4* mutations affecting splicing indirectly by inhibiting degradation of excised group I intron RNAs, which sequester tightly bound splicing factors (Turcq et al., 1992; Saldanha et al., 1995). Here, we cloned

[1]Correspondence: lambowitz@mail.utexas.edu

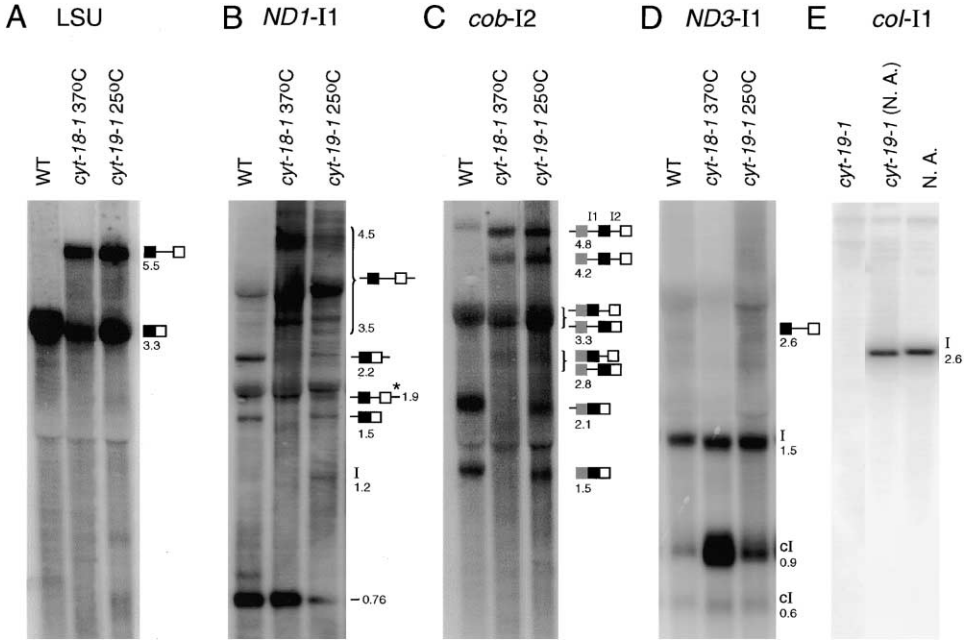

Figure 1. Northern Hybridizations

Northern blots of RNAs from wild-type 74*A* (WT) and the *cyt-18-1* and *cyt-19-1* mutants grown at their nonpermissive temperatures were hybridized with ^{32}P-labeled probes specific for the (A) *N. crassa* mt LSU, (B) *ND1*-I1, (C) *cob*-I2, and (D) *ND3*-I1 introns and flanking exons, and (E) group II intron *col*-I1 derived from the *N. crassa* natural isolate North Africa 430 (N.A.). Wild-type strains and *cyt-19-1* were grown at 25°C, and *cyt-18-1* was grown at 37°C. RNA species are identified to the right based on previous characterization of RNA processing pathways (Wallweber et al., 1997), with numbers indicating sizes (kb) relative to molecular weight markers (not shown); exons are indicated by filled or open boxes, and introns are indicated by lines between exons. The *ND1* and *cob* precursors have multiple 5′- and 3′-end processing steps, which are not distinguished. Abbreviations: I, intron; cI, circular intron; asterisk, alternatively spliced product of the *ND1* intron.

the *cyt-19* gene and show that it encodes a DEAD-box protein that functions in concert with CYT-18 to promote group I intron splicing by acting as an ATP-dependent RNA chaperone.

Results

Phenotype of the *cyt-19-1* Mutant

The *cyt-19-1* mutant was identified in a genetic screen of slowly growing, cytochrome-deficient (*cyt*) mutants, a phenotype indicative of defective mt gene expression (Bertrand et al., 1982). The mutant is partially cold sensitive. When grown at 25°C, *cyt-19-1* is deficient in cytochromes b and aa_3, while at 37°C, cytochrome b increases to wild-type levels but cytochrome aa_3 remains deficient. *N. crassa* mitochondria contain ten group I introns, of which three, the mt large subunit rRNA (LSU) intron, *ND1*-I1, and *cob*-I2, are dependent on the CYT-18 protein for splicing in vitro and in vivo (Wallweber et al., 1997). Most of the remaining group I introns contain a large "peripheral" RNA structure P5abc, which obscures the CYT-18 binding site and provides an alternate means of stabilizing the group I intron catalytic core (Mohr et al., 1994; Wallweber et al., 1997).

Figure 1 shows Northern hybridizations demonstrating that the *cyt-19-1* mutant grown at 25°C is defective in splicing all three CYT-18-dependent group I introns but is not defective in splicing the non-CYT-18-dependent group I intron *ND3*-I1 or the group II intron *col*-I1 found in a *N. crassa* natural isolate from North Africa (N.A.). The group I introns were monitored by using intron/exon probes, while the group II intron was monitored by using an intron probe to look for small amounts of unspliced precursor RNA. Northern hybridizations for additional group I introns showed that neither *cyt-18-1* nor *cyt-19-1* is defective in splicing *ND4*-I1, *ND4*L-I1, or *ND5*-I1, while both mutants are defective in splicing *ATPase6*-I1, *cob*-I1, and *ND5*-I2 (not shown). The latter three introns contain P5abc structures that may impede CYT-18 binding, and it is not clear whether the *cyt-18* and *cyt-19* mutations affect their splicing directly or indirectly—e.g., by inhibiting mt translation, which interferes with the synthesis of a required intron-encoded maturase (see Wallweber et al., 1997). In addition to the splicing defects, the *cyt-19-1* mutant is also defective in 5′-end processing of *cob* and *coII* pre-mRNAs, while 5′- and 3′-end processing of the mt rRNAs are unaffected (Henderson, 1981). The end processing defects in *cyt-19-1* are not found in *cyt-18* mutants and suggest that CYT-19 has at least one additional function besides RNA splicing.

Cloning of the *cyt-19* Gene

Because the *cyt-19-1* mutant has a leaky growth phenotype and the gene was missing from initially available *N. crassa* genomic libraries, we cloned the gene by chromosome walking (Figure 2 and Experimental Procedures). The chromosome walk identified a single cosmid (79F3 from the pLORISTH library) that maps 150–200 kb to the right of *arg-14* and complements the *cyt-19-1*

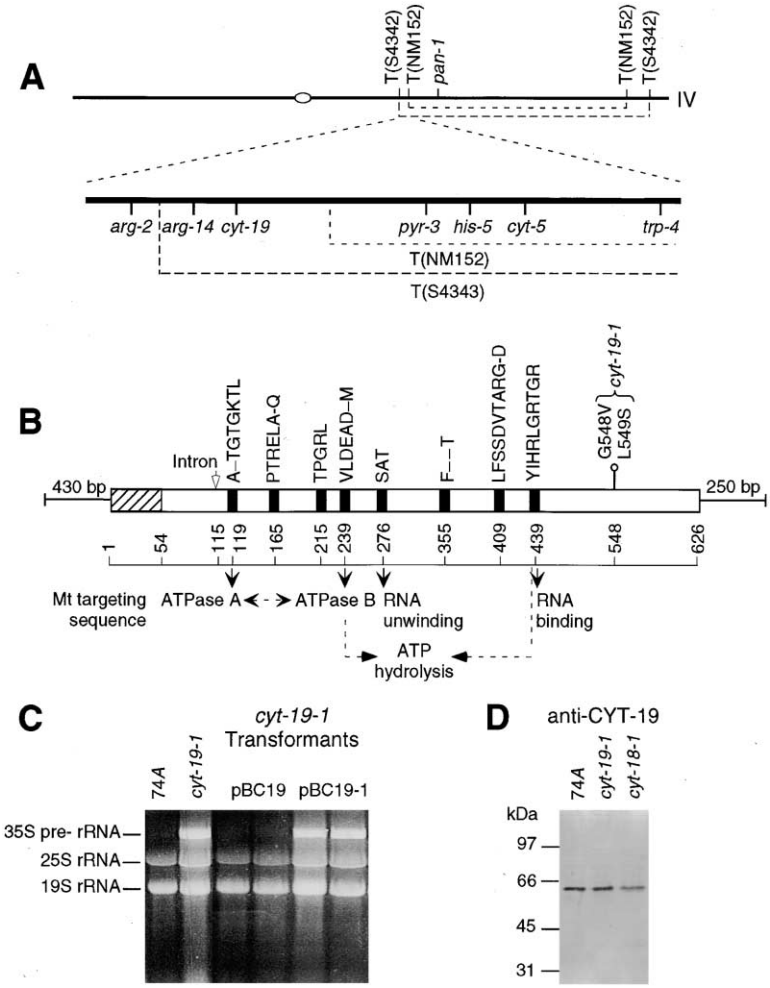

Figure 2. Cloning and Characterization of the *cyt-19* Gene

(A) Location of the *cyt-19* gene on linkage group IV. Crosses with strains containing translocated regions of linkage group IV showed that the *cyt-19* gene is included in the translocation T(S4343) but not T(NM152), and the location of *cyt-19* relative to *pyr-3*, *his-5*, *cyt-5*, and *trp-4* was determined by three-factor crosses. Chromosome walking identified a single cosmid 150–200 kb to the right of the *arg-14* that complements the *cyt-19-1* mutation.

(B) Map of the *cyt-19* gene. The gene encodes a 626 aa ORF with a putative 53 aa mt targeting sequence (hatched) and a 64 bp intron (open arrow). The ORF contains conserved amino acid sequence motifs characteristic of RNA-dependent ATPases (black bars with CYT-19 sequences indicated above and postulated functions below). The *cyt-19-1* mutant has amino acid substitutions G548V and L549S in the C-terminal region (open circle).

(C) Ethidium bromide-stained gel of mt RNAs from wild-type 74*A*, mutant *cyt-19-1*, and *cyt-19-1* transformed with pBC19 and pBC19-1, which contain wild-type and mutant *cyt-19* genes, respectively. RNA species are identified to the left.

(D) Immunoblots of mt proteins from the indicated strains probed with an anti-CYT-19 antibody preparation. After immunoblotting, the blots were stained with AuroDye to reveal other proteins and confirm equal loading. Molecular weight markers are indicated to the left.

mutation. A 2.5 kb DNA segment containing the wild-type *cyt-19* gene was subcloned from cosmid 79F3 into plasmid pBEN, which contains an *N. crassa* benomyl-resistance (Bn^R) marker, to generate plasmid pBC19. pBC19 fully complemented the growth, cytochrome, and splicing defects of the *cyt-19-1* mutant, whereas pBC19-1, which contains the corresponding DNA segment from the *cyt-19-1* mutant, did not complement the mutant phenotype (Figure 2C and not shown). These findings confirm that *cyt-19-1* is a recessive mutation, which results in loss or impairment of an activity required for efficient splicing of CYT-18-dependent group I introns in vivo.

Sequencing of pBC19 revealed that the *cyt-19* gene encodes a 626 aa ORF with DEAD-box and other motifs characteristic of ATP-dependent RNA helicases (Figure 2B; GenBank accession number AF497975). The ORF has a predicted 53 aa N-terminal mt targeting sequence and contains a 64 bp intron, whose position was confirmed by cDNA sequencing (not shown). Outside the conserved RNA helicase region, the ORF has no discernible sequence similarity to any other DExH/D-box protein. The *cyt-19-1* mutant allele has two amino acid changes, G548V and L549S, in the C-terminal region, with no other sequence changes in the remainder of the cloned 2.5 kb DNA segment, including 430 bp upstream and 250 bp downstream of the ORF. The sequences of the wild-type and mutant alleles were confirmed by direct sequencing of PCR products from genomic DNA. Immunoblots with anti-CYT-19 antibodies detected a single 63 kDa polypeptide present at similar levels in mt lysates of wild-type 74*A* and the *cyt-18-1* and *cyt-19-1* mutants (Figure 2D).

The CYT-19 Protein Has RNA-Stimulated ATPase Activity

The CYT-19 protein was synthesized in *E. coli* using an expression system in which the protein is linked to cleavable N- and C-terminal intein tags containing chitin binding domains to permit facile purification on a chitin-affinity column (see Experimental Procedures). Table 1 shows that the purified CYT-19 protein, like other DExH/D-box proteins involved in RNA transactions, has RNA-stimulated ATPase activity. In the case of CYT-19, the ATPase activity at saturating ATP and RNA concentrations was stimulated ~40-fold by group I or group II intron RNAs or by poly(C), stimulated less by poly(U) or poly(A), and inhibited by poly(G), poly(dA), or poly(dT). Steady-state kinetic analysis indicated that the RNA stimulation is due to an increase in k_{cat}, as found for other DExH/D-box proteins (see Table 1 legend; cf., Wagner et al., 1998). As expected, a mutation K125E in the ATPase

Table 1. The CYT-19 Protein Has RNA-Stimulated ATPase Activity

	ATP Hydrolysis ($\mu M/min^{-1}$)
CYT-19	0.06 ± 0.01
+poly(A)	1.1 ± 0.2
+poly(C)	2.3 ± 0.3
+poly(U)	1.1 ± 0.2
+poly(G)	$<10^{-3}$
+poly(dA)	0.002 ± 0.001
+poly(dT)	0.002 ± 0.001
+Group I intron RNA	2.7 ± 0.3
+Group II intron RNA	2.6 ± 0.2

ATPase activity was assayed at 25°C in 20 μl of splicing reaction medium containing 0.05 μM CYT-19, 10 μCi [γ-^{32}P]ATP (10 Ci/mmol) in the presence of saturating unlabeled ATP (1 mM) and RNA (1 μM for intron RNAs or 0.25 μg/μl for oligonucleotides). The table shows initial rates (r_0) corresponding to <1% final product in 100 min time courses; all reactions were linear for >15 min. The group I intron RNA was in vitro transcript pBD5a/BanI, which contains the *N. crassa* mini mt LSU intron and flanking exons, and the group II intron RNA was in vitro transcript pGMΔORF/BamHI, which contains a ΔORF-derivative of the *L. lactis* LI.LtrB intron (Saldanha et al., 1999). Saturation was confirmed by measuring r_0 at multiple ATP and RNA concentrations under each condition. Kinetic parameters were estimated by determining r_0 at saturating and subsaturating ATP (proportional to k_{cat} and k_{cat}/K_m, respectively; see Wagner et al., 1998). Addition of RNA had no significant effect on K_m [203 ± 46 μM (no additions), 190 ± 62 μM (group I intron), 204 ± 51 μM (group II intron), and 190 ± 58 μM (poly(C)], but substantially increased k_{cat} [1.2 ± 0.2 min^{-1} (no additions), 54 ± 6 min^{-1} (group I intron), 50 ± 4 min^{-1} (group II intron), and 46 ± 6 min^{-1} (poly(C)]. All values are the mean ± the standard deviation for three independent measurements.

active site eliminated ATPas activity under all conditions tested (not shown).

CYT-19 + ATP Stimulates Splicing of the *N. crassa* Mitochondrial LSU Intron at 25°C

We next tested whether the purified recombinant CYT-19 protein could stimulate the splicing of group I introns. First, we assayed splicing of the full-length 2.3 kb *N. crassa* mt LSU at different temperatures by addition of [^{32}P]GTP to the 5′ end of the excised intron (Figure 3A). As found previously (Guo et al., 1991), the LSU intron did not self-splice detectably at any temperature (lanes 1) but was spliced in the presence of the CYT-18 protein (lanes 2), and this CYT-18-dependent splicing was relatively efficient at 37°C but became progressively less efficient at lower temperatures. Significantly, the addition of CYT-19 + ATP greatly stimulated the inefficient CYT-18-dependent splicing reaction at 25°C and 30°C, but had relatively little effect on the more efficient reaction at 37°C (lanes 4). Controls showed that the stimulation by CYT-19 requires ATP (lanes 3) and that CYT-19 + ATP is unable to promote splicing in the absence of CYT-18 (lanes 5). These findings show that CYT-19 is required in addition to CYT-18 for efficient splicing of the full-length *N. crassa* mt LSU intron at 25°C, the normal growth temperature of *N. crassa*.

Kinetic Analysis of the Effect of CYT-19 on RNA Splicing

For more detailed analysis of the effect of CYT-19, we used a 388 nt derivative of the *N. crassa* mt LSU intron deleted for a large hairpin structure near the 5′ end of the intron and most of the ORF encoding mt ribosomal protein S-5 (Guo et al., 1991). The in vitro transcript pBD5a/BanI, which contains this mini-LSU intron with short flanking exons, is the standard substrate used in most previous CYT-18-dependent splicing experiments. Figure 3B shows time courses for splicing of the mini-LSU intron at 25°C, assayed using 20 nM ^{32}P-labeled RNA substrate and 100 nM protein. Under protein excess conditions, CYT-18-dependent splicing reactions are typically biphasic and a significant proportion of the RNA fails to splice even after prolonged incubation, due to the presence of slowly folding and inactive RNA conformers. At 25°C, the CYT-18-dependent splicing reaction was very slow ($k_1 = 4 \times 10^{-3}$ and $k_2 = 0.1 \times 10^{-3}$ min^{-1}, for the fast and slow phases, respectively) and less than 50% of the RNA was spliced at long time points, reflecting a high proportion of misfolded RNAs. Significantly, the addition of CYT-19 + ATP increased both k_1 and k_2 about 10-fold, dramatically increased the proportion of the RNA that spliced rapidly, and resolved inactive RNA conformers, so that essentially all of the RNA spliced at long time points. These effects were not observed for CYT-19 in the absence of ATP or in the presence of the nonhydrolyzable ATP analog AMP-PNP (Figure 3B) or for the CYT-19-1 or K125E mutant proteins (not shown). The results were essentially the same whether monitored by disappearance of precursor RNA or appearance of ligated exons (not shown). In addition to the *N. crassa* mt LSU intron, which belongs to structural subclass IA, CYT-19 + ATP also stimulated the CYT-18-dependent splicing of the *ND1* intron, a group IB intron, but had no effect on the self-splicing of the non-CYT-18-dependent group I introns *cob*-I1, *ND4*-I1, and *ND5*-I1 at 25°C (not shown).

CYT-19 Does Not Bind Specifically to Group I Intron RNAs and Does Not Affect the Binding of CYT-18

To investigate whether CYT-19 binds specifically to group I intron RNAs, we carried out equilibrium binding assays (Figure 4). In these experiments, low concentrations of ^{32}P-labeled RNA were incubated with increasing concentrations of CYT-19 protein and then filtered through nitrocellulose to retain RNA/protein complexes. CYT-19 by itself showed only very weak binding to the *N. crassa* mini-LSU or *ND3*-I1 group I introns, the *Lactococcus lactis* group II intron LI.LtrB, or poly(C), with no significant difference among the different RNAs (Figure 4A). Interestingly, the nonhydrolyzable ATP analog AMP-PNP increased the nonspecific binding of CYT-19 to all four RNAs (Figure 4A), whereas ATP, ADP, Pi, or ADP + Pi did not increase CYT-19 binding to any of the RNAs (Figure 4B and not shown). These findings indicate that CYT-19 does not bind specifically to group I intron RNAs but suggest that AMP-PNP may stabilize the protein in a conformation that has a higher nonspecific RNA binding affinity or increased retention on the filters.

Additional experiments showed that CYT-19 + ATP has no effect on the rate of binding of CYT-18 to the mini-LSU intron, whether added before or together with CYT-18, or on the dissociation rate of CYT-18/mini-LSU intron complexes (not shown; see Experimental Procedures). Further, RNA splicing assays carried out at RNA excess showed that CYT-19 + ATP does not increase

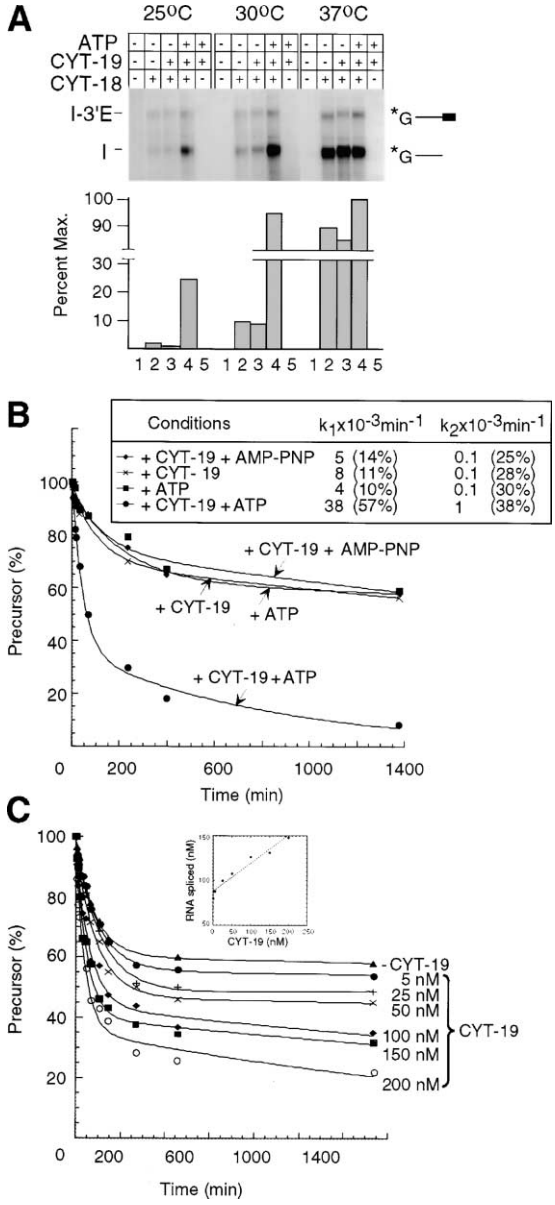

Figure 3. Effect of the CYT-19 Protein on In Vitro Splicing of the *N. crassa* Mitochondrial LSU Intron

(A) In vitro splicing of the full-length *N. crassa* mt LSU intron at different temperatures. Splicing reactions with 20 nM precursor RNA (in vitro transcript pHX11/EcoRI) and 100 nM of the indicated proteins were initiated with [^{32}P]GTP ± 1 mM ATP and incubated at different temperatures for 1 hr, a time verified to be in the linear range for all reactions. The products were separated in a 1.6% agarose gel and quantitated with a phosphorImager to detect the [^{32}P]GTP-labeled (asterisk) intron and I-3′E intermediate. The bar graphs show the percent of spliced intron relative to the maximum at 37°C in the presence of CYT-18 + CYT-19 + ATP.

(B) Effect of CYT-19 on CYT-18-dependent splicing of the mini-LSU intron at 25°C. Splicing reactions with 20 nM ^{32}P-labeled RNA (in vitro transcript pBD5a/BanI) and 100 nM CYT-18 ± 100 nM CYT-19 were initiated by the addition of 1 mM GTP ± 1 mM ATP or AMP-PNP, portions were removed at different times, and the products were analyzed in a denaturing 6% polyacrylamide gel. The plots show the rate of disappearance of precursor RNA as a function of time, with the data best fit to equations with two exponentials to obtain k_{obs} for the fast and slow phases (k_1 and k_2, respectively). The numbers in parentheses indicate the proportion of total RNA spliced in each phase.

(C) CYT-19 concentration dependence. Splicing time courses were carried out with the mini-LSU intron at 25°C, using 200 nM ^{32}P-labeled RNA, 200 nM CYT-18, and 5–200 nM CYT-19. The inset shows the amount of spliced RNA as a function of CYT-19 concentration.

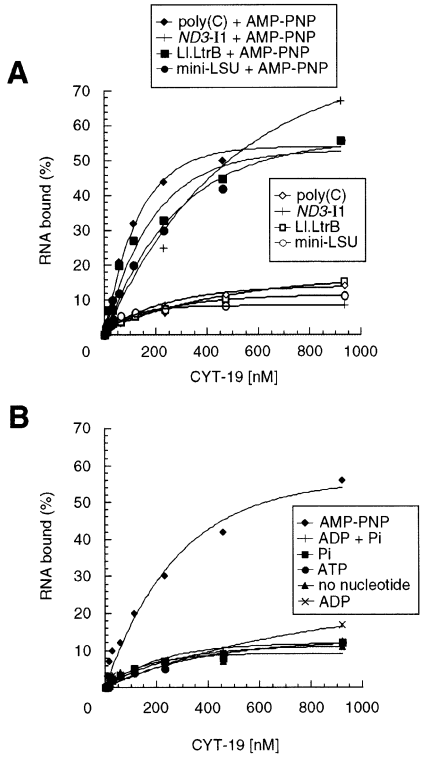

Figure 4. Equilibrium Binding Assays

The indicated ^{32}P-labeled RNAs (5 pM) were incubated with increasing concentrations of CYT-19 protein by itself or in the presence of 1 mM AMP-PNP (A) or ATP, ADP, Pi, or ADP + Pi (B) for 90 min at 25°C and then filtered through nitrocellulose to bind RNA/protein complexes. The plots show the percent of RNA bound as a function of CYT-19 concentration. Essentially the same curves were obtained for the mini-LSU, *ND3*-I1, and poly(C) with 60 or 90 min incubations, verifying that the binding was at equilibrium. We confirmed that binding did not increase at higher concentrations of AMP-PNP, ATP, ADP, or Pi.

the rate of turnover of CYT-18 from the excised intron RNA (not shown). We infer that CYT-19 acts at a step after CYT-18 binding and that the stimulation of splicing is not due to an increased rate of turnover of CYT-18 from the excised intron RNA.

CYT-19 Turns Over Slowly and May Function as a Multimer

To determine whether CYT-19 could facilitate multiple rounds of splicing, we carried out splicing reactions with the mini-LSU intron at 25°C with 200 nM ^{32}P-labeled RNA substrate plus 200 nM CYT-18 and increasing concentrations of CYT-19 from 5 to 200 nM (Figure 3C). The results showed that the amount of RNA spliced at long time points increased progressively with increasing con-

Table 2. Effect of CYT-19 on the Temperature Dependence of CYT-18-Dependent Splicing of the *N. crassa* Mini-LSU Intron

	Rate ($\times 10^{-3}$ min^{-1})			
	−CYT-19		+CYT-19	
Temperature	k_1	k_2	k_1	k_2
20°C	0.6 (15%)		15 (16%)	0.5 (30%)
25°C	5 (8%)	0.4 (24%)	25 (45%)	1.5 (30%)
30°C	24 (27%)	1.3 (31%)	60 (45%)	4.8 (40%)
37°C	86 (59%)	5.1 (27%)	102 (57%)	7.3 (29%)

Splicing time courses at different temperatures were initiated by addition of 100 nM CYT-18 ± 100 nM CYT-19 to equilibrated reaction medium containing 20 nM ^{32}P-labeled RNA (in vitro transcript pBD5a/BanI) and 1 mM GTP and ATP. The data were best fit to equations with one or two exponentials to obtain k_1 and k_2 for the fast and slow phases, respectively. The numbers in parentheses indicate the proportion of total RNA spliced in each phase.

centrations of CYT-19. Further, a plot of the amount of RNA spliced versus CYT-19 concentration was linear with a slope of 0.3 (Figure 3C, inset). These findings indicate that the rate of turnover of CYT-19 is substantially slower than the rate of splicing, so that CYT-19 acts on only one RNA substrate in vitro. Since CYT-19 carries out multiple rounds of ATP hydrolysis (Table I) and is stable for at least 3 hr under the conditions of the splicing assays (not shown), the most likely explanation is that CYT-19 remains associated with the group I intron/CYT-18 complex after splicing. The linear concentration dependence with a slope of 0.3 indicates either that CYT-19 functions as a multimer or that only ~30% of the protein is active.

Effect of CYT-19 + ATP on the Temperature Dependence of CYT-18-Dependent Splicing Reactions

The pronounced temperature dependence of CYT-18-dependent splicing reactions suggests that the rate-limiting step is likely to be a protein-induced RNA conformational change, which has a high activation enthalpy required to dissociate stable nonnative structures or intermediates (Webb et al., 2001). To investigate the effect of CYT-19 on this temperature dependence, we carried out kinetic analysis of the splicing of the mini-LSU intron at different temperatures after the addition of CYT-18 ± CYT-19 to equilibrated reaction medium containing precursor RNA and 1 mM GTP and ATP. As shown in Table 2, CYT-19 increased the rates of both the fast and slow phases, as well as the proportion of spliceable RNA, at all temperatures. However, the differential effect on the rates was progressively less at higher temperature, with CYT-19 having little effect on k_1 or k_2 at 37°C. Apparent activation enthalpies ($\Delta H^{\ddagger}$) calculated from the temperature dependence using plots of ln k versus 1/T were 56 ± 4 and 38 ± 4 kcal/mol for k_1 and k_2, respectively, and these decreased to 22 ± 3 and 24 ± 5 kcal/mol, respectively, in the presence of CYT-19. The results suggest that CYT-19 functions similarly to higher temperature to facilitate rate-limiting RNA structural transitions, which have a high activation enthalpy. Further, the CYT-19-mediated increases in k_1 and k_2 and the decrease in the fraction of inactive RNA suggest that CYT-19 facilitates at least three different structural transitions, each of which limits the rate of splicing for a fraction of the RNA population.

CYT-19 Disrupts Nonnative RNA Structures

To investigate directly how CYT-19 affects group I intron RNA structure, we first carried out chemical RNA structure mapping with the *N. crassa* mini-LSU intron. However, these experiments failed to detect a predominant nonnative structure trapped in the presence of CYT-18 at 25°C, likely reflecting the existence of multiple nonnative structures, none of which is sufficiently populated to be detected over background by chemical modification (not shown). We therefore turned to the *Tetrahymena* LSU intron, whose RNA folding pathway is characterized by the formation of a predominant nonnative secondary structure, denoted Alt-P3, which must dissociate prior to productive RNA folding (Pan and Woodson, 1998). As shown in Figure 5, the Alt-P3 structure forms when the P3[3′] sequence involved in the native P3 pairing mispairs with a sequence from J8/7.

The CYT-18 protein does not bind to the wild-type *Tetrahymena* LSU intron due to the presence of the large peripheral RNA structure P5abc, but it can functionally replace P5abc to promote splicing of a ΔP5abc-derivative of the *Tetrahymena* LSU intron at low Mg^{2+} concentrations (5 mM Mg^{2+}) (Mohr et al., 1994). Figure 5A shows that this CYT-18-dependent splicing of the ΔP5abc intron, monitored by the appearance of the excised intron, occurs slowly at 30°C, but both the rate and extent of splicing are dramatically increased by the addition of CYT-19 + ATP, as for the CYT-18-dependent *N. crassa* mt group I introns. The effect of CYT-19 + ATP is qualitatively similar when monitored by the disappearance of unspliced precursor RNA, but complicated because CYT-18-promoted splicing is accompanied by relatively rapid hydrolysis at the 3′ splice site, resulting in a nonproductive 5′E-I product (not shown). CYT-19 + ATP has no effect on self-splicing of the ΔP5abc intron at 15 mM Mg^{2+} (not shown). These results emphasize that both CYT-18 and CYT-19 can act on diverse group I introns.

To investigate the effect of CYT-19 + ATP on folding of the ΔP5abc RNA, we carried out DMS modification experiments at 5 mM Mg^{2+} in the presence and absence of CYT-18 and CYT-19 + ATP or AMP-PNP (Figure 5B). DMS methylates the N1 and N3 positions of unpaired A and C residues, respectively, leading to strong reverse transcription stops one base prior to the modified nucleotide residue. Using this reagent, the Alt-P3 and native P3 structures are readily distinguished by the status of four nucleotide residues in P3[5′], which are protected

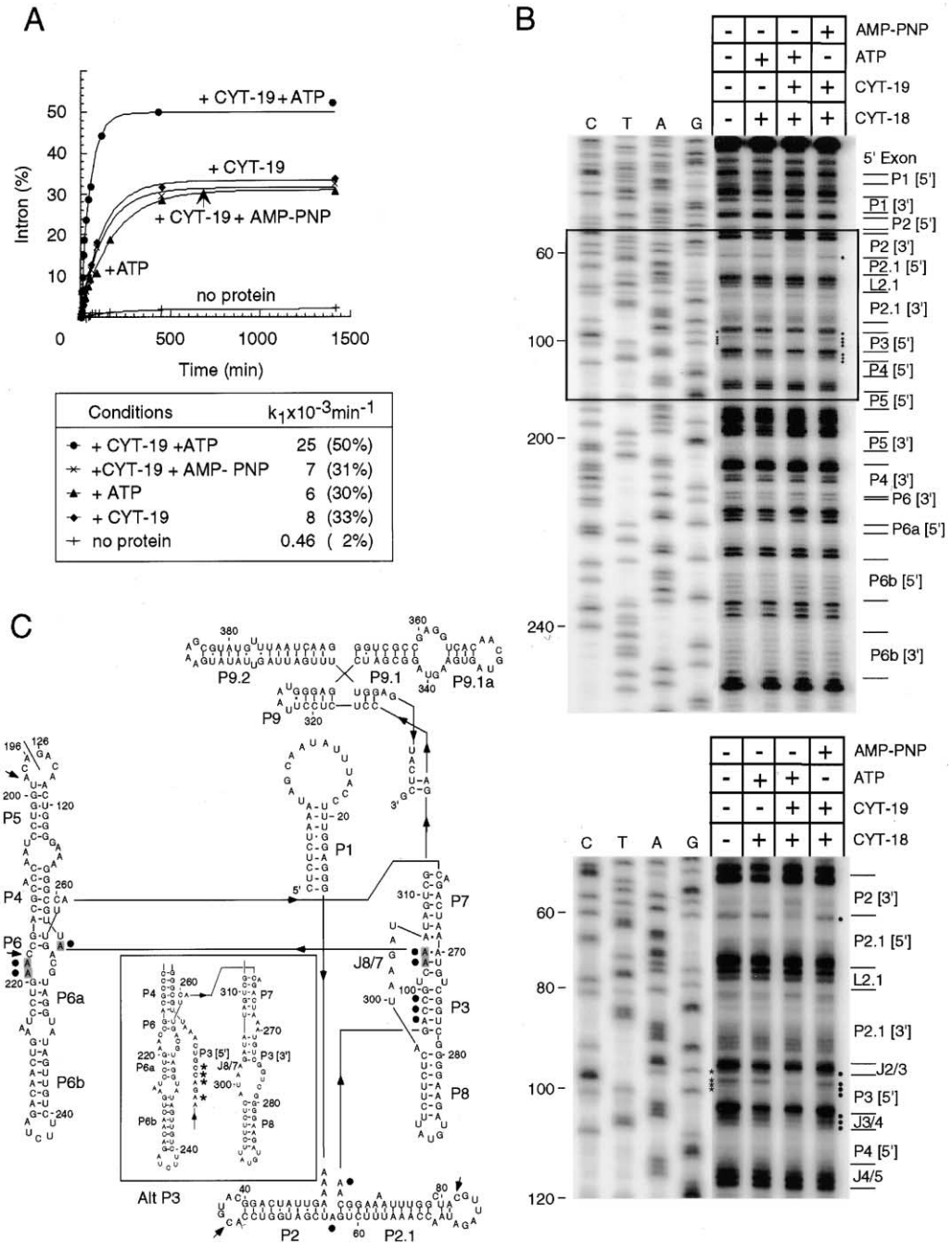

Figure 5. Effect of CYT-19 on the Splicing and Structure of the *Tetrahymena* ΔP5abc LSU Intron

(A) Splicing assays at 30°C were carried out as in Figure 3B, using 20 nM ^{32}P-labeled RNA and 100 nM CYT-18 ± 100 nM CYT-19 ± 1 mM ATP or 1 mM AMP-PNP. The plot shows the rate of appearance of the excised intron (% total counts) as a function of time.

(B) RNA structure mapping. 20 nM RNA was preincubated with 100 nM CYT-18 and CYT-19 plus 1 mM ATP or AMP-PNP and then modified with DMS. Modification sites were mapped by primer extension with M-MLV RT, using a 5′-labeled primer complementary to intron positions 274–298, and the gels were scanned with a phosphorImager for quantitation. The bottom shows an enlargement of the boxed region, which distinguishes P3 from Alt-P3. Lanes C, T, A, and G are dideoxy sequencing ladders obtained from pT7TT1A3ΔP5abc DNA using the same 5′-labeled primer. Intron positions are indicated to the left, and group I intron regions are indicated to the right.

(C) Predicted secondary structure of the *Tetrahymena* ΔP5abc intron and summary of DMS modifications and protections. The inset shows Alt-P3. Gray shading of nucleotide residues indicates ≥40% increased protection in the presence of CYT-18 compared to free RNA; closed circles indicate ≥40% increased protection after addition of CYT-19 + ATP; arrows indicate ≥50% increased modification after addition of CYT-19. Nucleotide residues that are base paired in the native P3 structure and unpaired in the Alt-P3 structure are indicated by asterisks.

by base pairing in the native P3 structure, but modified in the Alt-P3 structure (asterisks).

The DMS modification patterns show that the ΔP5abc RNA by itself forms most of the conserved group I intron secondary structure and that addition of CYT-18 results in the protection of a small number of additional bases in J3/4 and J6/6a (shaded), likely reflecting tertiary structure formation (see Mohr et al., 1994). As expected, the nonnative Alt-P3 structure was prominent in the RNA under these conditions. Significantly, CYT-19 + ATP almost completely converted Alt-P3 to the native P3 structure and also further enhanced the putative tertiary structure protections induced by CYT-18 in J3/4 and J6/6a. Neither of these effects were observed when CYT-19 was added together with the nonhydrolyzable ATP analog AMP-PNP. These findings demonstrate that CYT-19 acts as an RNA chaperone to disrupt a nonnative secondary structure that constitutes a kinetic trap in group I intron folding.

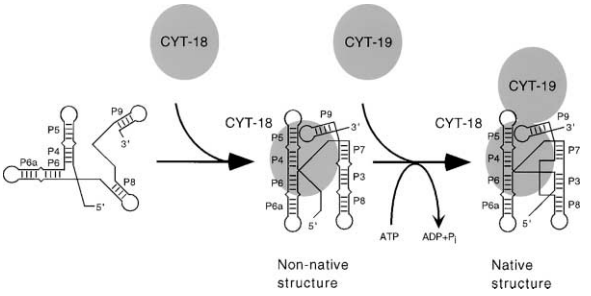

Figure 6. Model of CYT-18 and CYT-19 Function in Group I Intron Splicing

CYT-18 binds first to the P4-P6 domain to promote its assembly and then makes secondary contacts with the P3-P9 domain to stabilize interdomain interactions (Caprara et al., 1996a, 1996b; Myers et al., 2002). Because of the degeneracy of base pairing and tertiary interactions, the folded RNA has propensity to form a variety of stable nonnative structures, which constitute kinetic traps, and these are further stabilized by the tight binding of CYT-18 to the folded RNA, resulting in a high activation enthalpy for the final folding steps. CYT-19 alleviates these kinetic traps by using the energy of ATP hydrolysis to disrupt nonnative structures, enabling iterative refolding to the final native structure, which is stabilized by CYT-18.

Discussion

In the present work, we identified a DEAD-box protein, CYT-19, that functions in concert with the CYT-18 protein to promote group I intron splicing by acting as an ATP-dependent RNA chaperone. We showed first that a recessive mutation in the *cyt-19* gene inhibits the splicing of CYT-18-dependent group I introns in vivo. We then cloned the *cyt-19* gene and showed that the purified CYT-19 protein is required for efficient CYT-18-dependent group I intron splicing at physiological growth temperatures in vitro. CYT-19 does not bind specifically to group I intron RNAs and acts after CYT-18 binding to facilitate rate-limiting RNA structural changes, which have high activation enthalpies. Finally, we showed that CYT-19 can act on structurally diverse group I introns and functions as an RNA chaperone to resolve a prominent nonnative secondary structure, Alt-P3, which is a kinetic trap in the CYT-18-dependent splicing of the *Tetrahymena* ΔP5abc LSU intron. While other proteins have been suggested to function as RNA chaperones, CYT-19 is the first demonstrated to act directly at a specific step in RNA folding on a natural substrate.

The conclusive demonstration that CYT-19 acts as an RNA chaperone builds on extensive studies of the folding pathway of the *Tetrahymena* LSU intron (see Woodson, 2000). In the wild-type intron, which contains a large P5abc structure, the P4-P6 domain folds rapidly, while the P3-P9 domain folds more slowly because of a propensity to form nonnative secondary and tertiary structures, including Alt-P3, which must then rearrange to the native structure. Conditions that stabilize the folded RNA structure, including the presence of the P5abc structure or high Mg^{2+} concentrations, decrease the rate of splicing by stabilizing nonnative structures, whereas conditions that destabilize the folded RNA structure, including higher temperature, mild denaturants, or nonspecific RNA binding proteins, accelerate splicing, presumably by facilitating iterative refolding to the final native structure, which has the lowest free energy. This iterative refolding mechanism was first suggested by Karpel et al. (1982) to account for the ability of nonspecific RNA binding proteins to promote tRNA or 5S RNA renaturation, and it has since been invoked to account for the stimulatory effect of nonspecific RNA binding proteins on a variety of other RNAs, including group I introns (see Herschlag, 1995; Woodson, 2000). It has also been suggested as one possible mechanism by which the DExH/D-box protein Prp22p functions in nuclear pre-mRNA splicing (Wagner et al., 1998). Our findings for CYT-19 indicate that this predicted RNA chaperone function in group I intron folding requires a specific DEAD-box protein and is not fulfilled by generic nonspecific RNA binding proteins in vivo.

Considered together, our results suggest the model shown in Figure 6 for how CYT-18 and CYT-19 function together in group I intron splicing. Previous work indicated that CYT-18 binds first to the group I intron's P4-P6 domain to promote its assembly and then makes secondary contacts with the P3-P9 domain to stabilize interdomain interactions (Caprara et al., 1996a, 1996b). The role of CYT-18 in stabilizing the P4-P6 domain is equivalent to that of the P5abc structure in the *Tetrahymena* LSU intron (Mohr et al., 1994) and has the similar consequence of stabilizing nonnative RNA structures, resulting in an elevated activation enthalpy for the final folding steps. CYT-19 functions at this stage by using the energy of ATP hydrolysis to disrupt nonnative structures, enabling iterative refolding to the final native structure. The finding that CYT-19 does not turn over rapidly suggests that it may remain bound to the complex, albeit not required to maintain the final structure, which requires only CYT-18.

In addition to its RNA chaperone function, it remains possible that CYT-19 plays other roles, such as accelerating specific structural transitions or destabilizing inappropriate interactions between CYT-18 and the intron RNA. Further, most of our in vitro experiments were carried out with a streamlined mini-LSU intron substrate and not with the full-length precursor RNA, which may additionally depend on CYT-19 to resolve a competing large hairpin structure near the 5′ splice site and/or more

extensive nonnative interactions involving the full-length exons and intron ORF (Wollenzien et al., 1983). We note that the *cyt-19-1* mutant remains partially defective in splicing the mt LSU intron in vivo, even at 37°C, possibly reflecting the greater difficulty of folding the full-length precursor RNA.

CYT-19 appears remarkably specific in facilitating the splicing of only CYT-18-dependent group I introns. One possible explanation is that the CYT-18-dependent introns are simply more dependent on an RNA chaperone because CYT-18 binding exacerbates kinetic traps. Recent studies have shown that the yeast bI5 intron can be spliced either by its normal splicing factor, the yeast CBP2 protein, using a tertiary structure-capture mechanism, or by the CYT-18 protein, using a tertiary structure-induction mechanism (Webb et al., 2001). The substitution of CYT-18 for CBP2 changes the rate-limiting step from one with a low activation enthalpy to one with a high activation enthalpy, likely due to the stabilization of nonnative RNA structures in the folding pathway. Thus, the apparent specificity of CYT-19 could simply reflect that RNA chaperone-facilitated refolding is rate limiting for the splicing of CYT-18-dependent introns, but not other group I introns. This explanation begs the question of whether the non-CYT-18-dependent group I introns are dependent on other tightly binding splicing factors, such as maturases, which would similarly exacerbate kinetic traps.

An alternate possibility is that CYT-19 is targeted to group I introns by interaction with CYT-18 or with a folded RNA structure induced by CYT-18 binding. Consistent with this possibility, the finding that CYT-19 does not turn over rapidly suggests that it may remain associated with the complex even after splicing. The *E. coli* DExH/D-box protein DbpA appears to be targeted to its site of action by binding to a specific hairpin structure in 23S rRNA, while other DExH/D box proteins may be targeted by interaction with partner proteins in RNP complexes (see Tanner and Linder, 2001). The interaction of CYT-19 with the folded RNA and/or CYT-18 would presumably tether it in position to nonspecifically disrupt nonnative secondary or tertiary structures in the partially folded intron RNAs.

In addition to being defective in RNA splicing, the *cyt-19-1* mutant is defective in a subset of 5′-end-processing reactions (Henderson, 1981). These 5′-end-processing defects likely reflect an additional function of the CYT-19 protein, since they are not observed in *cyt-18* mutants and are thus unlikely to be secondary effects of defective RNA splicing or mt protein synthesis. CYT-19 may also function in translation or other processes. As for other DExH/D-box proteins, it will be of interest to determine how the different functions of CYT-19 are targeted or regulated.

With respect to evolution, we suggested previously that group I introns were dispersed relatively recently as mobile elements and became dependent on preexisting cellular proteins, such as the mt TyrRS, as a result of mutations that impaired self-splicing (Lambowitz and Perlman, 1990). Consistent with a recent evolutionary origin, the cellular proteins that function in group I intron splicing differ, even in closely related organisms, and in a number of cases include proteins that function specifically in splicing only one or a small number of related group I introns. As discussed above, the recruitment of tightly binding protein factors to promote splicing has the deleterious consequence of exacerbating kinetic traps, necessitating the recruitment of RNA chaperones for efficient splicing. It seems likely that CYT-19 was a preexisting DEAD-box protein that functioned in other processes, such as 5′-end processing, and was then recruited to function in group I intron splicing. Mirroring the idiosyncratic nature of the splicing factors, different RNA chaperones may have been similarly recruited to facilitate group I and group II intron splicing in other organisms. The yeast protein Mss116p is a second DExH/D-box protein that could potentially function as an RNA chaperone. If so, its targeting appears different from CYT-19, since mutations in Mss116p result in defective splicing of both group I and group II introns (Séraphin et al., 1989).

Finally, the demonstration that a DExH/D-box protein is required as an RNA chaperone in group I intron splicing supports the possibility that dedicated RNA chaperones are similarly required in vivo for the folding of other and perhaps all large RNAs and shows that these proteins can be identified genetically, despite the background of cellular nonspecific RNA binding proteins. CYT-19 should now provide an excellent model system for studying the mechanism by which DExH/D-box proteins mediate RNA conformational changes on natural substrates and how such proteins are targeted to function in specific processes.

Experimental Procedures

N. crassa Strains and Growth Conditions

N. crassa strains were wild-type 74-OR23-1*A* (denoted 74*A*), *cyt-18-1 al-2* (299-9 RAC *al-2 a*), and *cyt-19-1 pan-2 a* (Bertrand et al., 1982). A *cyt-19-1* strain containing the *col*-I1 group II intron was constructed by crossing *cyt-19-1* with the group II intron-containing strain North Africa Adiopodoume (FGSC 430, mating type *A*) as the female parent. Genetic methods and growth of cells in liquid culture were as described (Davis and de Serres, 1970; Bertrand et al., 1982).

Cloning of the *cyt-19* Gene

The *cyt-19* gene was cloned by chromosome walking from the *cyt-5* and *arg-14* genes using three cosmid libraries (pSV50, pMOCOSX, and pLORISTH) and a YAC library obtained from the Fungal Genetics Stock Center (Kansas City, KA). Cosmids identified in the chromosome walk were tested for complementation of the *cyt-19-1* mutation by standard *N. crassa* transformation procedures (Akins and Lambowitz, 1985). Transformants were selected by hygromycin- or benomyl-resistance markers on the vector and then tested for rescue of the mutant's growth and RNA splicing defects at 25°C.

cyt-19 Clones and Expression Constructs

pBC19 and pBC19-1 contain the wild-type and mutant *cyt-19* genes, respectively, cloned in pBEN (previously denoted pBML), a pBS(+)-based plasmid containing an *N. crassa* benomyl-resistance (*Bn*^{r}) marker (Turcq et al., 1992). To construct pBC19 and pBC19-1, the *cyt-19* and *cyt-19-1* genes were PCR amplified from *N. crassa* wild-type 74*A* or *cyt-19-1* DNA using VENT polymerase (New England Biolabs, Beverly, MA) with primers H70 (5′-GCTCTAGAATGTACCG TAAGGTAGCTCATCCC) and H2000 (5′-GCTCTAGAACAACAAGC CACCCCAATGTATGG), which add XbaI sites. The resulting 2.5 kb PCR products were then cloned into the XbaI site of pBEN.

pETC-19 contains a 574 aa ORF encoding the wild-type CYT-19 protein cloned downstream of the phage T7 promoter in pET-11c (Novagen, Madison, WI). The ORF lacks the predicted mt targeting sequence but has an extra N-terminal ATG for expression in *E. coli*. pTWC19 and pTWC19-1 contain the corresponding wild-type and

mutant *cyt-19* ORFs fused to N- and C-terminal intein tags containing chitin binding domains in pTWIN1 (New England Biolabs). pTWC19 was constructed via PCR of the CYT-19 ORF from pETC-19 with primers that add a SapI site for cloning into the SapI site of pTWIN1. pTWC19-1 was constructed similarly by PCR of *cyt-19-1* DNA, with an additional round of PCR, using primers that delete the intron. The CYT-19 K125E mutant was constructed in pTWIN1 by PCR-mediated mutagenesis. All *cyt-19* constructs were sequenced completely.

Purification of the CYT-18 and CYT-19 Proteins

The CYT-18 protein was expressed in *E. coli* from plasmid pEX560 and purified as described (Saldanha et al., 1995). Wild-type and mutant CYT-19 proteins were expressed and purified using the pTWIN constructs (see above). After transforming the constructs into *E. coli* HMS174(DE3), cells were grown at 25°C to $OD_{595} = 0.5$ and induced with 1 mM IPTG for 20 hr. The cells were then harvested by centrifugation and lysed by three cycles of freeze/thawing in the presence of 10 μg/ml lysozyme. The expressed CYT-19 protein was purified from the lysate by using a chitin-affinity column, followed by intein cleavage, according to the manufacturer's protocol, except that 500 mM KCl was used in place of 500 mM NaCl. The preparations gave a single band in Coomassie blue-stained polyacrylamide gels, with an average yield of 5 mg/l culture. The protein was stable for at least 3 months when stored at 4°C in 50% glycerol.

Northern Hybridizations

Whole-cell RNA was denatured with glyoxal, run in a 1.4% agarose gel, blotted to Hybond-N (Amersham), and hybridized with ^{32}P-labeled probes (Wallweber et al., 1997). Group I intron probes were ^{32}P-labeled antisense transcripts containing the intron and flanking exons transcribed from the following recombinant plasmids digested with restriction enzymes: mt LSU intron, pBD5a/PvuII; *ND1*-I1, pND15′E/PstI; *ND3*-I1, pND3/EcoRI; and *cob*-I2, pcobI-2/HindIII (Wallweber et al., 1997). A probe for the *col*-I1 group II intron was generated by PCR of the North Africa strain DNA using a 5′ primer corresponding to intron positions 6–33 and a 3′ primer complementary to positions 3016–3060. The PCR product was labeled with [α-^{32}P]dCTP (3000 Ci/mmol; NEN Life Science Products, Boston, MA) by random priming using a RadPrime kit (Invitrogen, Carlsbad, CA).

Immunoblotting

Immunoblotting was as described by Turcq et al. (1992). Blots of mt proteins separated in an 8% polyacrylamide-SDS gel were probed with rabbit antibodies raised against gel-purified CYT-19 expressed from pETC-19 in *E. coli* BL21 (Bethyl Laboratories, Montgomery, TX).

ATPase Assays

ATPase activity was assayed by monitoring [γ-^{32}P]ATP hydrolysis using thin-layer chromatography (Wagner et al., 1998). After the reactions, the plates were dried and quantitated with a phosphorImager.

RNA Splicing Assays

RNA substrates were synthesized by in vitro transcription using T3 or T7 Megascript or Maxiscript kits (Ambion, Austin, TX), with [α-^{32}P]UTP added to synthesize ^{32}P-labeled RNAs. The full-length *N. crassa* mt LSU intron was transcribed from BamHI-digested pHX11 to yield a 3.2 kb RNA containing an 818 nt 5′ exon, the 2.3 kb intron, and a 56 nt 3′ exon (Akins and Lambowitz, 1987). The 388 nt ΔORF ("mini") mt LSU intron was transcribed from BanI-digested pBD5a to yield a 503 nt RNA containing a 65 nt 5′ exon, the 388 nt intron, and a 50 nt 3′ exon (Guo et al., 1991). Transcripts containing other group I or group II introns were synthesized from the following recombinant plasmids digested with restriction enzymes: *ND1*-I1 and *ND3*-I1, pND1m/NdeI and pND3/XbaI, respectively (Wallweber et al., 1997); *Tetrahymena* ΔP5abc LSU intron, pT7TT1A3ΔP5abc/EcoRI (Mohr et al., 1994); *L. lactis* LI.LtrB group II intron, pGMΔORF/BamHI (Saldanha et al., 1999).

In vitro splicing reactions were carried out with specified amounts of ^{32}P-labeled precursor RNAs and 1 mM GTP or with unlabeled precursor RNA and 0.2 mM [α-^{32}P]GTP (0.1 Ci/mmol) in 100 mM KCl, 5 mM $MgCl_2$, 25 mM Tris-HCl (pH 7.5) (Saldanha et al., 1995). Prior to use, RNAs were renatured by heating to 92°C for 2 min and cooling on ice, and then warmed to reaction temperature in splicing buffer alone or with specified amounts of the CYT-18 and/or CYT-19 proteins. Splicing reactions were incubated as described for individual experiments and terminated by adding an equal volume of 0.1 M EDTA, 0.2 M Tris-HCl (pH 7.5), followed by extraction with phenol-chloroform-isoamyl alcohol (25/24/1; phenol-CIA). Where indicated, 1 mM ATP or the nonhydrolyzable ATP analog AMP-PNP (adenylyl-imidodiphosphate; Roche, Indianapolis, IN) were added together with GTP. RNAs were analyzed in either 1.6% agarose gels (full-length mt LSU intron) or denaturing 6% polyacrylamide gels (all other introns), which were dried and quantitated with a PhosphorImager.

RNA Binding Assays

RNA binding assays were carried out at 25°C as described (Saldanha et al., 1995), except that nitrocellulose filter binding was done with a 96-well minifold (Schleicher and Schuell, Keene, NH), and the nitrocellulose membrane was backed by a Hybond-N membrane (Amersham, Piscataway, NJ) to bind free RNA, enabling normalization for different inputs. To measure association rates, 5 pM ^{32}P-labeled in vitro transcript pBD5a/BanI (29 Ci/mmol) was incubated with 700 pM CYT-18 ± 700 pM CYT-19 in reaction medium containing 1 mM ATP. To measure dissociation rates, complexes were formed between 20 nM ^{32}P-labeled pBD5a/BanI RNA and 10 nM CYT-18 in reaction medium containing 1 mM ATP, followed by addition of 10 nM CYT-19. Portions were removed at the indicated times and mixed with an equal volume of splicing buffer containing 1 mg/ml heparin to bind unassociated protein, prior to filtration.

DMS Modification

DMS modification experiments were done with 20 nM RNA and 100 nM proteins in 400 μl of 100 mM KCl, 5 mM $MgCl_2$, and 10 mM HEPES-KOH, pH 7.5 (Caprara et al., 1996b). After preincubation for 30 min at 30°C, modification reactions were initiated by adding DMS (1:500 final dilution), incubated for 5 min, and terminated by adding 5 μl of 14.3 M β-mercaptoethanol and 8 μl 200 mM EDTA plus 10 μg *E. coli* tRNA carrier, followed by phenol-CIA extraction and two ethanol precipitations. These conditions gave less than one modification per RNA. Modification sites were mapped by primer extension with M-MLV RT (Invitrogen), using 5′-labeled primers complementary to different regions of the intron RNA. The primer extension products were analyzed in a denaturing 6% polyacrylamide gel, which was dried and quantitated with a PhosphorImager. Modifications and protections were assigned based on the change in band intensity relative to a reference lane (see Figure 5).

Acknowledgments

We thank Jonathan Arnold for the pLORISTH cosmid library, Daniela Roy for technical assistance, and Georg Mohr, Roland Saldanha, Rick Russell, Ken Johnson, and Dan Herschlag for comments on the manuscript. This work was supported by National Institutes of Health grant GM37951.

Received: January 30, 2002
Revised: May 8, 2002

References

Akins, R.A., and Lambowitz, A.M. (1985). General method for cloning *Neurospora crassa* nuclear genes by complementation of mutants. Mol. Cell. Biol. *9*, 2272–2278.

Akins, R.A., and Lambowitz, A.M. (1987). A protein required for splicing group I introns in *Neurospora* mitochondria is mitochondrial tyrosyl-tRNA synthetase or a derivative thereof. Cell *50*, 331–345.

Bertrand, H., Bridge, P., Collins, R.A., Garriga, G., and Lambowitz, A.M. (1982). RNA splicing in *Neurospora* mitochondria. Characterization of new nuclear mutants with defects in splicing the mitochondrial large rRNA. Cell *29*, 517–526.

Caprara, M.G., Lehnert, V., Lambowitz, A.M., and Westhof, E. (1996a). A tyrosyl-tRNA synthetase recognizes a conserved tRNA-

like structural motif in the group I intron catalytic core. Cell *87*, 1135–1145.

Caprara, M.G., Mohr, G., and Lambowitz, A.M. (1996b). A tyrosyl-tRNA synthetase protein induces tertiary folding of the group I intron catalytic core. J. Mol. Biol. *257*, 512–531.

Clodi, E., Semrad, K., and Schroeder, R. (1999). Assaying RNA chaperone activity *in vivo* using a novel RNA folding trap. EMBO J. *13*, 3776–3782.

Coetzee, T., Herschlag, D., and Belfort, M. (1994). *Escherichia coli* proteins, including ribosomal protein S12, facilitate in vitro splicing of phage T4 introns by acting as RNA chaperones. Genes Dev. *8*, 1575–1588.

Davis, R.H., and de Serres, F.J. (1970). Genetic and microbiological research techniques for *Neurospora crassa*. Methods Enzymol. *27A*, 79–143.

Golden, B.L., Gooding, A.R., Podell, E.R., and Cech, T.R. (1998). A preorganized active site in the crystal structure of the *Tetrahymena* ribozyme. Science *282*, 259–264.

Guo, Q., Akins, R.A., Garriga, G., and Lambowitz, A.M. (1991). Structural analysis of the *Neurospora* mitochondrial large rRNA intron and construction of a mini-intron that shows protein-dependent splicing. J. Biol. Chem. *266*, 1809–1819.

Henderson, M.F. (1981). The effect of *cyt-4–1*, *cyt-18–1* and *cyt-19–1* mutations on RNA processing in *Neurospora* mitochondria. Master's thesis, Saint Louis University, St. Louis, Missouri.

Herschlag, D. (1995). RNA chaperones and the RNA folding problem. J. Biol. Chem. *270*, 20871–20874.

Jankowsky, E., Gross, C.H., Shuman, S., and Pyle, A.M. (2000). The DExH protein NPH-II is a processive and directional motor for unwinding RNA. Nature *403*, 447–451.

Jankowsky, E., Gross, C.H., Shuman, S., and Pyle, A.M. (2001). Active disruption of an RNA-protein interaction by a DExH/D RNA helicase. Science *291*, 121–125.

Karpel, R.L., Miller, N.S., and Fresco, J.R. (1982). Mechanistic studies of ribonucleic acid renaturation by a helix-destabilizing protein. Biochemistry *21*, 2102–2108.

Lambowitz, A.M., and Perlman, P.S. (1990). Involvement of aminoacyl-tRNA synthetases and other proteins in group I and group II intron splicing. Trends Biochem. Sci. *11*, 440–444.

Lambowitz, A.M., Caprara, M.G., Zimmerly, S., and Perlman, P.S. (1999). Group I and group II ribozymes as RNPs: clues to the past and guides to the future. In The RNA World, 2nd ed., R.F. Gesteland, J.F. Atkins, and T.R. Cech, eds. (Cold Spring Harbor, New York: Cold Spring Harbor Press), pp. 451–485.

Mannella, C.A., Collins, R.A., Green, M.R., and Lambowitz, A.M. (1979). Defective splicing of mitochondrial rRNA in cytochrome-deficient nuclear mutants of *Neurospora crassa*. Proc. Natl. Acad. Sci. USA *76*, 2635–2639.

Michel, F., and Westhof, E. (1990). Modelling of the three-dimensional architecture of group I catalytic introns based on comparative sequence analysis. J. Mol. Biol. *216*, 585–610.

Mohr, G., Caprara, M.G., Guo, Q., and Lambowitz, A.M. (1994). A tyrosyl-tRNA synthetase can function similarly to an RNA structure in the *Tetrahymena* ribozyme. Nature *370*, 147–150.

Myers, C.A., Kuhla, B., Cusack, S., and Lambowitz, A.M. (2002). tRNA-like recognition of group I introns by a tyrosyl-tRNA synthetase. Proc. Natl. Acad. Sci. USA *99*, 2630–2635.

Niemer, I., Schmelzer, C., and Börner, G.V. (1995). Overexpression of DEAD box protein pMSS116 promotes ATP-dependent splicing of a yeast group II intron *in vitro*. Nucleic Acids Res. *23*, 2966–2972.

Pan, J., and Woodson, S.A. (1998). Folding intermediates of a self-splicing RNA: mispairing of the catalytic core. J. Mol. Biol. *280*, 597–609.

Saldanha, R.J., Patel, S.S., Surendran, R., Lee, J.C., and Lambowitz, A.M. (1995). Involvement of *Neurospora* mitochondrial tyrosyl-tRNA synthetase in RNA splicing. A new method for purifying the protein and characterization of physical and enzymatic properties pertinent to splicing. Biochemistry *34*, 1275–1287.

Saldanha, R., Chen, B., Wank, H., Matsuura, M., Edwards, J., and Lambowitz, A.M. (1999). RNA and protein catalysis in group II intron splicing and mobility reactions using purified components. Biochemistry *38*, 9069–9083.

Séraphin, B., Simon, M., Boulet, A., and Faye, G. (1989). Mitochondrial splicing requires a protein from a novel helicase family. Nature *337*, 84–87.

Tanner, N.K., and Linder, P. (2001). DExD/H box RNA helicases: from generic motors to specific dissociation functions. Mol. Cell *8*, 251–262.

Turcq, B., Dobinson, K.F., Serizawa, N., and Lambowitz, A.M. (1992). A protein required for RNA processing and splicing in *Neurospora* mitochondria is related to gene products involved in cell cycle protein phosphatase functions. Proc. Natl. Acad. Sci. USA *89*, 1676–1680.

Wagner, J.D., Jankowsky, E., Company, M., Pyle, A.M., and Abelson, J.N. (1998). The DEAH-box protein PRP22 is an ATPase that mediates ATP-dependent mRNA release from the spliceosome and unwinds RNA duplexes. EMBO J. *17*, 2926–2937.

Wallweber, G.J., Mohr, S., Rennard, R., Caprara, M.G., and Lambowitz, A.M. (1997). Characterization of *Neurospora* mitochondrial group I introns reveals different CYT-18 dependent and independent splicing strategies and an alternative 3′ splice site for an intron ORF. RNA *3*, 114–131.

Webb, A.E., Rose, M.A., Westhof, E., and Weeks, K.M. (2001). Protein-dependent transition states for ribonucleoprotein assembly. J. Mol. Biol. *309*, 1087–1100.

Wollenzien, P.L., Cantor, C.R., Grant, D.M., and Lambowitz, A.M. (1983). RNA splicing in *Neurospora* mitochondria: structure of the unspliced 35S precursor ribosomal RNA detected by psoralen cross-linking. Cell *32*, 397–407.

Woodson, S.A. (2000). Recent insights on RNA folding mechanisms from catalytic RNA. Cell. Mol. Life Sci. *57*, 796–808.

Zhang, A., Derbyshire, V., Galloway Salvo, J.L., and Belfort, M. (1995). *Escherichia coli* protein StpA stimulates self-splicing by promoting RNA assembly *in vitro*. RNA *1*, 783–793.